ELSEVIER

Biochimica et Biophysica Acta 1511 (2001) 381–390

BIOCHIMICA ET BIOPHYSICA ACTA
BBA

www.bba-direct.com

Stretch-sensitive switching among different channel sublevels of an endothelial cation channel

Xiaoqiang Yao *, Hiu-Yee Kwan, Yu Huang

Department of Physiology, Faculty of Medicine, Chinese University of Hong Kong, Hong Kong, PR China

Received 17 July 2000; received in revised form 6 February 2001; accepted 13 February 2001

Abstract

A mechanosensitive Ca^{2+}-permeable cation channel was recorded by patch clamp in isolated rat aortic endothelial cells. A low level of channel activity could be observed after seal formation. The channel displayed some inward rectification and had a conductance for inward current of approx. 32 pS in Ca^{2+}-free pipette and bath solutions. Negative suction of −10 to −20 mmHg increased the probability of the channel being open. When the negative pressure in the pipette was raised to −35 to −45 mmHg, the channel underwent an abrupt transition to a large conductance substate that was interrupted occasionally by two other low conductance levels. Under this condition, the overwhelming majority of openings and closings were between a main level of 83 pS and the closed level. Compared to the 32 pS substate, the 83 pS large conductance substate had shorter mean open and closed times. The two channel substates had similar ionic selectivity and both were sensitive to the inhibition of cGMP and protein kinase G. This is the first demonstration showing that mechanostress can change the single channel conductance level of an ion channel in eukaryotic cells.

Keywords: Mechanosensitive cation channel; Conductance substate; Calcium; Protein kinase G; Nitric oxide; Guanosine monophosphate, cyclic

1. Introduction

Mechanosensitive Ca^{2+}-permeable channels have previously been reported in vascular endothelial cells [1–5]. These channels are suggested to be mechanotransducers, which transform the mechanical signal of blood flow into the chemical signal of intracellular Ca^{2+} level. Blood flow may open these mechanosensitive channels, resulting in a subsequent rise in $[Ca^{2+}]_i$. The increase in $[Ca^{2+}]_i$ then leads to the activation of a Ca^{2+}-sensitive constitutive form of nitric oxide synthase, which catalyzes the production of nitric oxide [6,7]. The elevation of $[Ca^{2+}]_i$ may also stimulate the production and release of PGI_2 [8] and endothelial-derived hyperpolarizing factor (EDHF) [9]. Nitric oxide, PGI_2, and EDHF are important endothelial factors that can modulate vascular tone and blood pressure [9].

In general, mechanosensitive channels respond to mechanical stress by altering the probability of the channel being open. The ion selectivity and conductance of biological channels are generally not mechanosensitive [10]. The only published exception is alamethicin, which is an antibiotic produced by fungus *Trichoderma viride*. Alamethicin aggregates on the membrane to form multimeric channels with multiple

* Corresponding author. Fax: +86-852-260-350-22; E-mail: yao2068@cuhk.edu.hk

0005-2736/01/$ – see front matter
PII: S0005-2736(01)00300-5

conductance substates [11]. Applied membrane tension leads to the switching of the channel among multiple conductance substates [12]. Bedard and Morris have also reported a stretch-activated chloride channel displaying multiple subconductances in helix snail neurons [13]. Mechanical stretch causes transition of the chloride channel from inactive to active mode. However, it is not clear whether the transitions among different substates of this chloride channel are also mechanical sensitive [13].

We have previously reported a mechanosensitive Ca^{2+}-permeable channel in vascular endothelial cells. It was a nonselective cation channel displaying inward rectification with slope conductance for inward current at 32 pS in Ca^{2+}-free pipette and bath solutions. The activity of this channel was regulated by protein kinase G [14]. In the present study, we report that under a strong negative pressure this mechanosensitive channel displays multiple subconductance levels with the predominate sublevel at approx. 83 pS.

2. Materials and methods

2.1. Materials

Active protein kinase G (a bovine recombinant isoform 1α), 8-Br-cGMP, cGMP and KT5823 were obtained from Calbiochem (USA). Primary antibody against von Willebrand factor and FITC-labeled secondary antibody were from Dako (Denmark). Culture media RPMI, FBS and PBS were supplied by Gibco-BRL (USA). EGTA, EDTA, ATP, trypsin and collagenase were purchased from Sigma (USA).

2.2. Preparation of aortic endothelial cells

Primary aortic endothelial cells were isolated from rat aorta and cultured as described elsewhere [15]. Briefly, male Sprague-Dawley rats were decapitated. The thoracic aorta was removed and washed twice with sterile PBS. Fat and connective tissues were then trimmed off. The aorta was cut into small sheets and treated with 0.2% collagenase in PBS for 15 min at 37°C. The suspension after the enzyme digestion was centrifuged at $800 \times g$ for 5 min. The cells were resuspended in 90% RPMI and 10% FBS, and then kept in an incubator at 37°C.

2.3. Cell culture

The isolated aortic endothelial cells were cultured in 90% RPMI 1640 and 10% FBS. The cells were incubated in T-25 tissue culture flasks in air with 5% CO_2 atmosphere at 37°C. Confluent cell monolayers were passaged using 0.25% trypsin containing 2.5 mM EDTA. The isolated aortic endothelial cells displayed a typical oblong morphology in cultured medium for up to the fourth passage. Only cells from the first two passages were used for the experiments.

2.4. Immunofluorescence

The identity of the primary cultured rat aortic endothelial cells was confirmed by immunostaining using an antibody against von Willebrand factor. The cultured cells were fixed in 4% formaldehyde in PBS for 2 h, and blocked with 1% BSA in PBS for 30 min. The cells were then stained with a polyclonal antibody against human von Willebrand factor (diluted 1/400 in PBS with 1% BSA) overnight at 4°C. The slides were then washed in PBS, and then incubated with FITC-labeled goat anti-rabbit IgG for 1 h. Slides were counterstained with 0.00003% DAPI in 0.9% NaCl. For controls, some slides were incubated in 1% BSA in PBS without the primary antibody. After washing in PBS, the slides were mounted in glycerol and examined under a fluorescence microscope. Counting the cells from five different slides containing more than 500 cells per slide yielded the conclusion that $96 \pm 2\%$ ($n = 5$) of the isolated cells were of endothelial origin. Specificity of the antibody was confirmed by the fact that it stained the endothelium layer but not the smooth muscle layers in tissue sections of rat aorta.

2.5. Single channel recording

Single channel currents were measured by standard methods [14,16] with an EPC-9 patch clamp amplifier. The patch pipettes have a tip diameter of about 1 μm. The signal was sampled at 5.0 kHz and filtered at 1 kHz for data analysis. Data were analyzed by TAC and TAC-fit software. The probability of the channel being open (NP_o) was estimated from the total time spent in the open state divided by the total

time of the record. A continuous recording of 5 s was used to estimate NP_o values. Negative pressure (suction) was applied to the patch pipettes using a syringe. A H_2O manometer was used to monitor the pipette pressure.

2.6. Solutions

Ca^{2+} saline contained in mM: 100 $CaCl_2$, 10 HEPES, pH 7.4. Because of the pH adjustment, Ca^{2+} saline actually contained 4.5 mM sodium ion. Na^+-glutamate solution contained in mM: 142.5 Na^+-glutamate, 1 EGTA, 10 HEPES, pH 7.4; NaCl saline contained in mM: 140 NaCl, 2.5 KCl, 1 EGTA, 10 HEPES, pH 7.4; KCl saline contained in mM: 140 KCl, 2.5 NaCl, 1 $CaCl_2$, 10 HEPES, pH 7.4. NaOH or KOH was used to adjust the pH of all solutions. Vehicle contained 10 μM cGMP, 10 μM ATP and 7 mM $MgCl_2$. They were required for activation of protein kinase G [17]. Vehicle was added prior to the addition of active protein kinase G. The results were presented as mean ± S.E.M. (*n*). All experiments were conducted at room temperature.

3. Results

3.1. The mechanosensitivity of the channel

Patch clamp experiments were used to identify nonselective cation channels sensitive to mechanical stimulation. Inside-out membrane patches were obtained with NaCl saline in the pipette and KCl saline in the bath. The patch's potential was held at −60 mV, which was close to its resting membrane potential [14]. Immediately after formation of inside-out membrane patches, we observed a low level of channel activity in about 30% of membrane patches. The channel displayed inward rectification with a slope conductance for inward current at approx. 32 pS. When a negative pressure of −10 to −20 mmHg was applied to the pipette, the channel activity in-

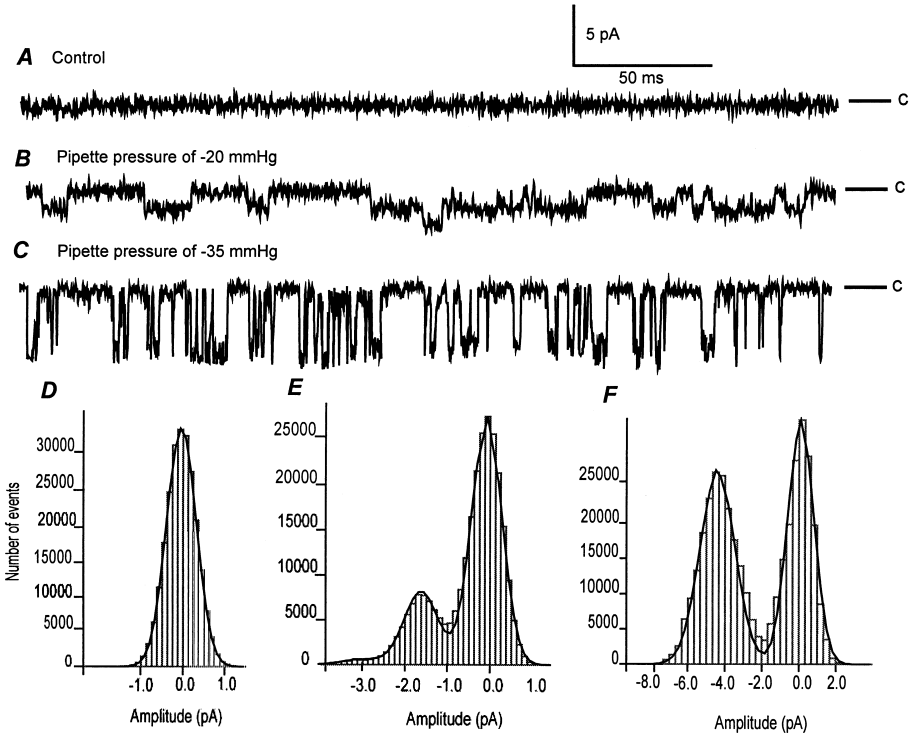

Fig. 1. Activation of a nonselective cation channel by mechanostretch in a representative inside-out membrane patch. The pipette/bath solutions contained NaCl saline/KCl saline. (A–C) Single channel current traces. (E,F) Current amplitude histograms for A–C. Each histogram was derived from current activities during a period of 30 s. (A,D) Control; (B,E) a negative pipette pressure of −20 mmHg; (C,F) a negative pipette pressure of 35 mmHg. The patch potential was held at −60 mV. All the traces were obtained from a single membrane patch. The closed level is marked by c.

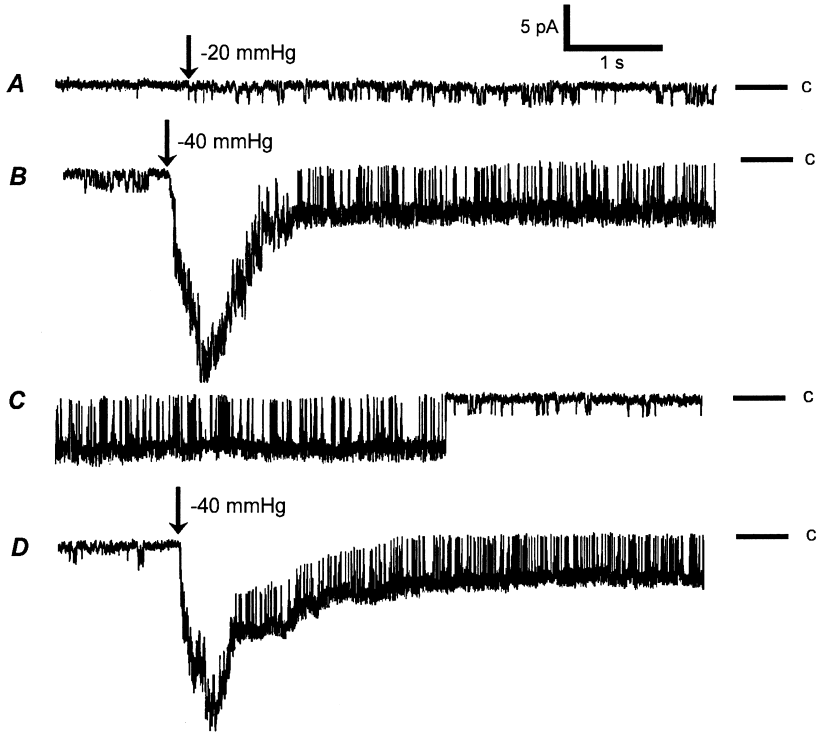

Fig. 2. Stretch-induced transition among different channel sublevels in a cell-attached patch. The pipette/bath solutions contained NaCl saline/KCl saline. (A) A negative pipette pressure of −20 mmHg activates a low conductance substate. (B) A subsequent suction of −40 mmHg activates a high conductance channel substate. (C) Reappearance of the low conductance substate after inactivation of the large conductance substate. (D) Suction reactivates the large conductance substate. The closed level is marked by c.

creased drastically while the channel conductance remained constant (Fig. 1B). The mean NP_o value for 60 s period increased from 0.005 ± 0.01 to 0.15 ± 0.05 ($n = 16$). When the pipette pressure was raised to −35 to −45 mmHg, there was a large transient inward current. After the current stabilized, a large conductance substate became clearly visible (Fig. 2B). There were flickering transitions between the large conductance substate and the closed state (Fig. 1C). The mean NP_o value of the large conductance substate was 0.76 ± 0.06 ($n = 6$).

Fig. 1 illustrates the typical steady state recordings of two channel substates with different thresholds of activation. The mechanosuction-caused current transitions are displayed in Fig. 2A,B. It appeared that the transition between the low and the high conductance substates was abrupt and behaved like an 'all or none' phenomenon dependent upon whether the pressure threshold was reached. A sustained stretch at low pressure of −20 mmHg would not cause transition from the low to the high conductance substate.

Careful inspection of the current traces revealed

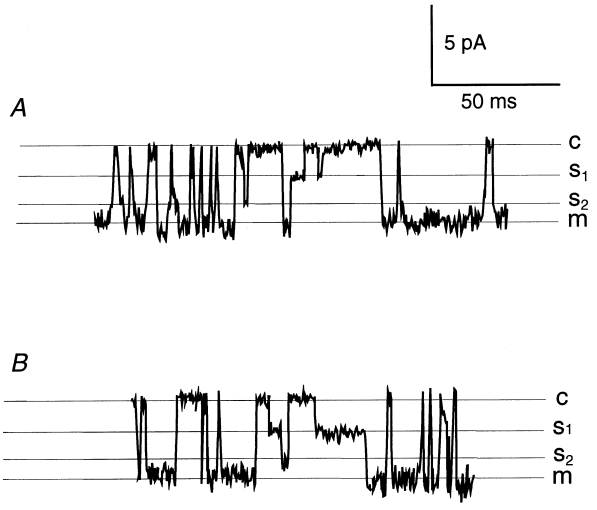

Fig. 3. Conductance levels of a channel under a high negative pressure of −40 mmHg. Multiple sublevels can be seen. A and B represent two separate current traces recorded in inside-out membrane patches. The pipette/bath solutions contained NaCl saline/KCl saline. The closed level is marked by c, the main level by m, and the other two sublevels by s_1 and s_2.

that, under high negative pressure, the large conductance substate was interrupted occasionally by two other low conductance levels (s_1 and s_2) (Fig. 3A,B). It appeared that s_1 corresponded to the 32 pS substate that was active before the strong suction of −35 to −45 mmHg. It should be emphasized that, under the strong suction, the overwhelming majority of openings and closings were between a main level of 83 pS and the closed level (Fig. 1C). The events of s_1 substate were very few and could only be spotted occasionally. The events of s_2 substate were even fewer. These are reflected in the event histograms in Fig. 1F, in which no other subconductance levels can be discerned.

We studied the time response of the channel activities to mechanical stimulation. Although mechanical suction activated (turned on) both 83 pS and 32 pS substates with no apparent time delay, removal of mechanical suction did not inactivate the channels immediately in either excised or cell-attached patches. Both channel substates maintained their activities for a long period of time. For the small conductance substate, the activity lasted for 18.5 ± 2.6 min ($n = 22$), whereas the large conductance substate lasted for 15.2+3.5 min ($n = 12$). The closing of the 83 pS large conductance substate was followed by reappearance of the 32 pS small conductance substate (Fig. 2C). A subsequent suction could reactivate the 83 pS large conductance substate (Fig. 2D).

3.2. Dwell time distribution

The single channel kinetics of both channel substates were investigated. Results from a typical ex-

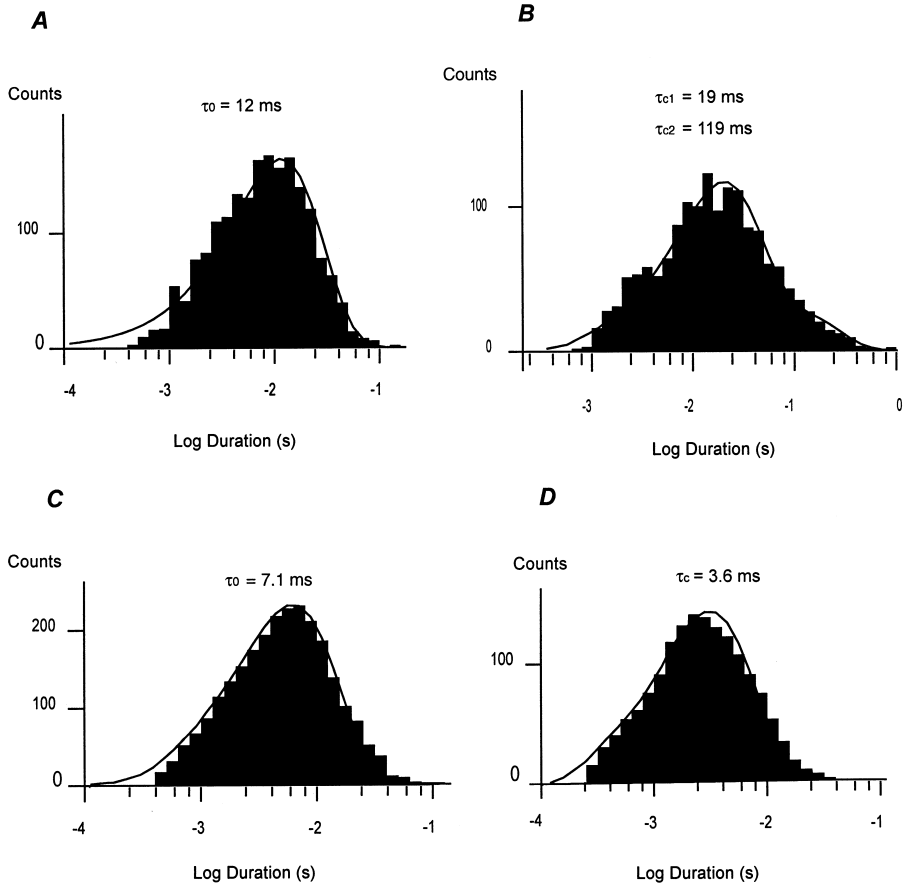

Fig. 4. Duration histograms of mechanosensitive cation channels. (A) Open time duration histogram of the small conductance substate; (B) closed time duration histogram of the small conductance substate; (C) open time duration histogram of the large conductance substate; (D) closed time duration histogram of the large conductance substate. All the data were generated from a single inside-out patch. Each histogram was derived from current activities during a period of 30 s. (A,B) Negative pipette pressure of −20 mmHg. (C,D) Negative pipette pressure of −40 mmHg. The patch potential was held at −60 mV.

periment are shown in Fig. 4. Under a negative pressure of −20 mmHg, the 32 pS substate could be observed. Open time distribution of the 32 pS substate could be well fitted by a single exponential component (Fig. 4A) with mean open time being $\tau_o = 14 \pm 1$ ms ($n = 5$). Closed time distribution could be fitted by the sum of two exponential curves (Fig. 4B) with mean closed times being $\tau_{c1} = 17 \pm 1$ ms and $\tau_{c2} = 125 \pm 3$ ms respectively ($n = 5$). Under a pipette pressure of −40 mmHg, the 83 pS substate appeared. The 83 pS substate had much shorter open and closed times. Both open time distribution and close time distribution could be fitted with one exponential curve (Fig. 4C,D). The mean open time was 7.6 ± 0.4 ms ($n = 4$) and the mean closed time was 3.4 ± 0.2 ms ($n = 4$). For both substates, open time and closed time distributions were voltage independent.

3.3. Relative permeability of two conductance substates to different cations

Both conductance substates demonstrated some inward rectification. When the pipette solution contained NaCl saline and the bath solution contained KCl saline, single channel conductance for the small conductance substate was calculated to be 32 ± 3 pS and E_{Rev} was 0 ± 0.1 mV ($n = 6$) (Fig. 5). For the large conductance substate, the respective values were 83 ± 4 pS ($n = 5$) and 0 ± 5 mV ($n = 5$) (Fig. 5). Since the reversal potentials were near zero, the channel should be equally permeable to K^+ and Na^+. This conclusion was further confirmed by the observation that change of the pipette/bath solutions from NaCl saline/KCl saline to KCl saline/NaCl saline had no effect on either slope conductance or reversal potential.

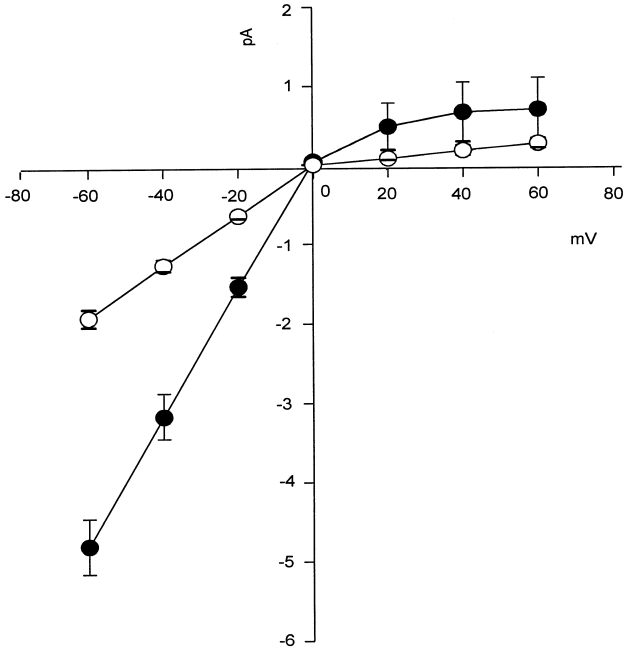

Fig. 5. Single channel current-voltage relationships of two channel substates. I-V relationships were obtained from inside-out patches. The pipette/bath contained NaCl saline/KCl saline. ○, the small conductance activity under a negative pipette pressure of −20 mmHg; ●, the large conductance activity under a negative pipette pressure of −40 mmHg. Mean ± S.E.M. ($n = 5$).

To estimate the relative permeability to Ca^{2+}, we recorded the single channel currents with the pipette solution being Ca^{2+} saline and the bath solution being Na^+-glutamate. For the small conductance substate, g was 9 ± 2 pS and E_{Rev} was 20 ± 4 mV ($n = 4$). For the large conductance substate, the current signals became very flickering when the pipette contained a high concentration of Ca^{2+}. It was difficult to accurately estimate the current amplitude of a single channel. Therefore we were not able to obtain a reasonable estimation of single channel conductance. The reversal potential was estimated to be 25 ± 4 mV ($n = 5$). Based on the reversal potential measurements, it was estimated that, for the small conductance substate, $P_{Ca}:P_{Na}:P_K = 5:1:1$, and for the large conductance substate, $P_{Ca}:P_{Na}:P_K = 7:1:1$ [18,19]. No measurable change either in conductance or in reversal potential was observed when Cl^- in the bath was replaced by glutamate, suggesting that this channel was not permeable to Cl^-.

3.4. Effect of cGMP and KT5823 on the 83 pS large conductance substate

We reported previously that the small conductance substate was sensitive to the inhibition by cGMP and protein kinase G [14]. Here we tested the effect of protein kinase G activator or inhibitor on the large conductance substate. The large conductance substate was first activated by a pipette pressure of −35 to −45 mmHg. Application of 8-Br-cGMP, a membrane-permeant activator of protein kinase G, almost completely abolished the activity of the large conductance substate in cell-attached membrane patches (Fig. 6). 8-Br-cGMP (1 mM) reduced the

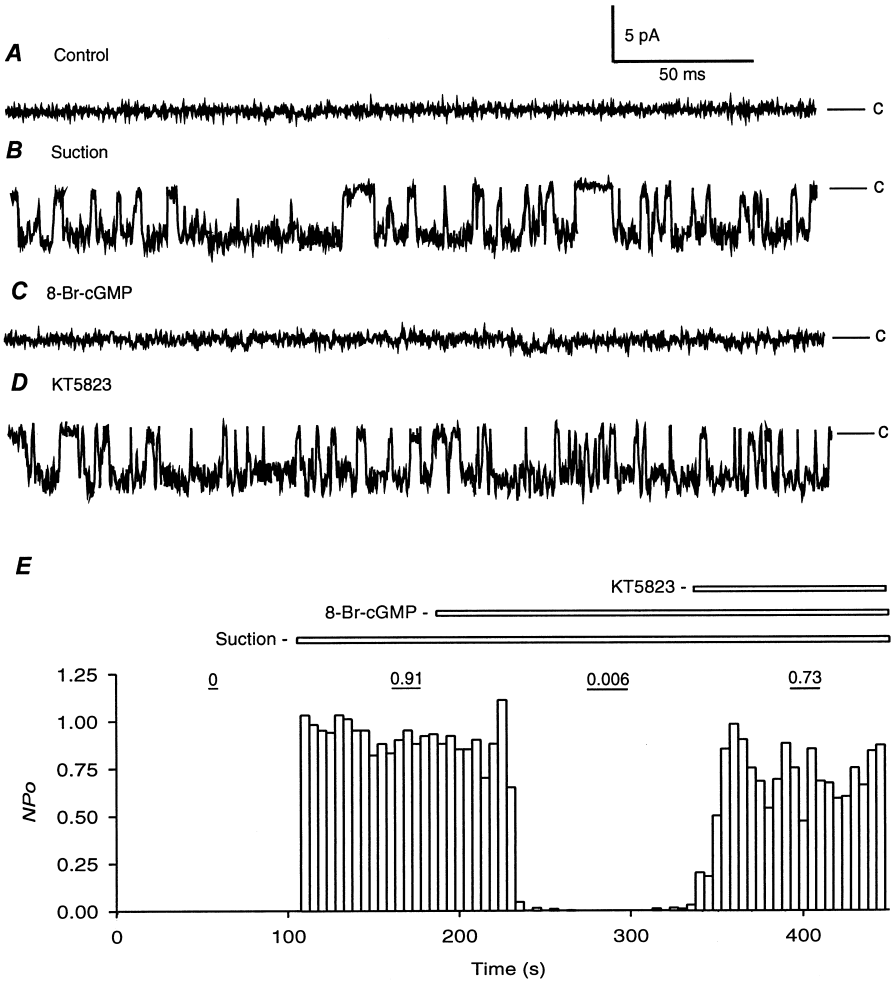

Fig. 6. Effect of 8-Br-cGMP and KT5823 on the large conductance substate in a representative cell-attached patch. The patch potential was −40 mV displaced from its resting potential. The pipette/bath contained NaCl saline/KCl saline. (A–D) Single channel current traces. (A) Control; (B) a suction of −35 mmHg; (C) 1 mM 8-Br-cGMP in the presence of suction; (D) 1 μM KT5823 in the presence of 1 mM 8-Br-cGMP and suction; (E) NP_o values of the above patch in 5 s intervals. The average NP_o values are displayed on the top. The closed level is marked by c.

mean NP_o values from 0.73 ± 0.06 ($n = 5$) to 0.02 ± 0.01 ($n = 5$). As illustrated in Fig. 6, the inhibitory effect could only be observed about 1 min after application of 8-Br-cGMP to the bath. This time lag could probably be explained by diffusion of the chemical to the cytoplasmic side under the patch pipettes. Subsequent application of KT5823 (1 μM), a potent and specific inhibitor of protein kinase G, reversed the inhibitory effect of 8-Br-cGMP with NP_o values increasing from 0.02 ± 0.01 ($n = 4$) to 0.57 ± 0.06 ($n = 4$). These results suggest that the activity of the large conductance substate is regulated by protein kinase G. We also tested the effect of the active form of protein kinase G in inside-out patches. Similar to what we found for the small conductance substate [14], treatment of exogenous protein kinase G (10 nM) abolished the activity of the large conductance substate (data not shown). Taken together, these results suggest that, like the 32 pS small conductance substate, the 83 pS large conductance substate is also inhibited by protein kinase G via a phosphorylation-dependent mechanism.

4. Discussion

Endothelial cells lining the inner surface of blood vessels are constantly exposed to hemodynamically

imposed mechanostress. These cells are able to sense the mechanical forces generated by blood flow, and in response synthesize and release potent vasodilators [20]. Although the underlying mechanisms of flow-induced vasodilation remain elusive, one possibility is that flow may cause an increase in $[Ca^{2+}]_i$ [6,7,14,21–23]. With the use of patch clamp technique, we recorded a mechanosensitive Ca^{2+}-permeable channel in isolated rat aortic endothelial cells. This channel demonstrates inward rectification with slope conductance for inward current at about 32 pS in Ca^{2+}-free pipette and bath solutions. Mechanostress leads to changes in both the single channel conductance and the single channel open probability. A negative pressure of −10 to −20 mmHg increases the open probability of the small conductance substate whereas a considerable larger pressure of −35 to −45 mmHg promotes the transition of the channel from a 32 pS small conductance substate to a multiple subconductance state with the predominate sublevel at approx. 83 pS. The 83 pS large conductance substate also has considerable higher channel open probability. The mechanosensitive switches among different sublevels may allow the cells to elegantly sense and respond to subtle changes in blood flow. As a result, the magnitude of Ca^{2+} influx may match well with the magnitude of mechanical stimulation. A greater mechanostress may translate into a higher rate of Ca^{2+} influx. The change in intracellular Ca^{2+} level may then trigger other signal transduction processes, leading to alterations in production and release of vasoactive agents such as nitric oxide, endothelium-derived hyperpolarizing factor, and PGI_2.

It is possible that the so-named two channel substates may actually represent two distinct types of channels. However, this hypothesis is unlikely since we have not seen any superposition of two conductance levels even under a more negative pipette pressure of −40 mmHg. Moreover, there seems to be an abrupt transition of conductance level triggered by more negative pipette pressure. High negative pressure first triggers a large transient current. After the current stabilizes, an 83 pS large conductance substate clearly dominates. This large transient current is not caused by a transient change in seal resistance, since the same pressure step does not cause a transient current in the patches that do not contain a stretch channel. Pressure-induced transient current has been reported previously by Hamill and McBride [24]. The transient current is likely caused by the pressure-induced opening of multiple channels followed by an adaptation of channel current. In our cases, however, this 'adaptation of the channel current' is very brief since NP_o stabilizes in approx. 1–2 s. A second possibility is that the transient current may be actually caused by a second rapidly adapting channel, but the fact that the transient current and the 83 pS substate always appear together in the same patches makes the first possibility more likely. The suspicion can be raised that the high conductance substate may be the result of mechanical damage of the patches under strong mechanical stretch [25], but this is unlikely since the high conductance substate preserves its ion selectivity. In addition, the activity of the large conductance substate channel can be abolished by the application of cGMP or active protein kinase G.

We studied the time response of the channels to mechanical stimulation. Although mechanical suction activated (turned on) both channel substates with no apparent time delay, removal of mechanical suction did not inactivate the channels immediately. The channel maintained its activity for a long period of time. This type of slow inactivation of the mechanosensitive channel upon suction release was reported previously by Bedard and Morris for a stretch-activated Cl^- channel in snail neurons, although the time duration of the activity in their case was much shorter (in the range of 10–15 s) [13]. Mechanical stretch has also been reported to cause irreversible activation of the *Xenopus* oocyte MS channel [24]. More recently, Tabarean et al. [26] showed that sodium channels could undergo an irreversible change in their inactivation kinetics as a result of mechanical stretch. The inactivation properties of the channel we reported here appear to lie in between the above-mentioned Cl^- channel in snail neurons and the MS channel in *Xenopus* oocytes. The endothelial mechanosensitive cation channel is reversible but with a prolonged time delay. One possible explanation for this long delay in inactivation is the pressure-associated changes in patch structure. Pressure can cause deformation of the membrane or travel of the sealed region along the pipette wall, resulting in changes in membrane tension to

activate the channels [27]. The resulting membrane deformation may not be rapidly reversed by removal of mechanical stress [10,27]. In agreement with this, we found that the channel activity elicited by negative suction could be abolished by a subsequent positive pressure in the pipette. An alternative explanation is that the mechanical stretch may cause some changes in channel structure that may not be readily reversible. The third possibility for this long delay in inactivation is that the channel could be modulated by a membrane-bound mechanosensitive enzyme [10]. In other words, the channel gating itself may not be mechanosensitive. Instead, the channel activity may be modulated by a mechanosensitive enzyme.

Nitric oxide is a crucial component in the cardiovascular system. An abnormal regulation in nitric oxide production may cause malfunction in the regulation of vascular tone [7]. An excessive cellular nitric oxide may also harm endothelial cells, resulting in apoptosis and cell death [28,29]. Therefore, it is conceivable that vascular endothelial cells may need an elaborate and well-refined regulatory system for the fine control of cellular levels of Ca^{2+} and nitric oxide. We have previously suggested that the mechanosensitive Ca^{2+}-permeable channel could be a crucial component in the regulation of the intracellular Ca^{2+} level [14]. It may allow Ca^{2+} influx to be finely regulated dependent upon the production of nitric oxide and cGMP. The present study demonstrates that a mechanosensitive Ca^{2+}-permeable channel in vascular endothelial cells displays mechanosensitive switching among different channel substates. cGMP and PKG can inhibit the activity of the 83 pS as well as the 32 pS substate. These channel properties may help the endothelial cells to finely regulate their intracellular levels of Ca^{2+} and nitric oxide.

Some caution will have to taken when linking the mechanosensitive properties of the channel to its physiological role, especially for the 83 pS large conductance substate. The large conductance substate can only be seen after a large transient current that is elicited by a substantial stretch. Higher stretch may deliver more traumas to patch membrane and result in decoupling of the membrane-cytoskeleton interactions [24,30]. Normal endothelial cells in physiological condition may never experience such a traumatized tension. On the other hand, however, our recent data indicated that the mechanosensitivity of Ca^{2+} influx into endothelial cells could be greatly enhanced under some physiological conditions such as in the presence of agonist ATP or bradykinin (unpublished results), suggesting that the mechanosensitivity of the endothelial cation channel could be much higher under certain physiological conditions.

In conclusion, we have found that a mechanosensitive Ca^{2+}-permeable cation channel displays stretch-sensitive switches among different substates. A higher mechanical tension promotes the transition of the channel from a small conductance substate to a large conductance substate. To our knowledge, this is the first report showing that mechanostress can alter the single channel conductance level of an ion channel in eukaryotic cells.

Acknowledgements

This study was supported by grants from the Hong Kong Research Grant Council (CUHK 4079/00M).

References

[1] J.B. Lansman, T.J. Hallam, T.J. Rink, Single stretch-activated ion channels in vascular endothelial cells as mechanotransducers?, Nature 325 (1987) 811–813.
[2] R. Popp, J. Hoyer, J. Meyer, H.J. Galla, H. Gogelein, Stretch-activated non-selective cation channels in the antiluminal membrane of porcine cerebral capillary, J. Physiol. 454 (1992) 435–449.
[3] J. Hoyer, A. Distler, W. Hasse, H. Gogelein, Ca^{2+} influx through stretch-activated cation channels activates maxi K^+ channels in porcine endocardial endothelium, Proc. Natl. Acad. Sci. USA 91 (1994) 2367–2371.
[4] J. Hoyer, R. Kohler, W. Hasse, A. Distler, Up-regulation of pressure-activated Ca^{2+}-permeable cation channel in intact vascular endothelium of hypertensive rats, Proc. Natl. Acad. Sci. USA 93 (1996) 11253–11258.
[5] S.M. Marchenko, S.O. Sage, Effect of shear stress and changes in osmolarity on endothelium of rat aorta, J. Physiol. 506 (1998) 17P.
[6] J. Ando, A. Ohtsuka, R. Korenaga, I. Sakuma, A. Kamiya, Flow-induced calcium transients and release of endothelium-derived relaxing factor in cultured vascular endothelial cells, Front. Med. Biol. Eng. 5 (1993) 17–21.
[7] A. Kanai, H.C. Strauss, G.A. Truskey, A.L. Crews, S. Grunfeld, T. Malinski, Shear stress induces ATP-independent transient nitric oxide release from vascular endothelial cells, measured directly with porphyrinic microsensor, Circ. Res. 77 (1995) 284–293.

[8] M. Hecker, A. Mulsch, F. Bassenge, R. Busse, Vasocontraction and increased flow: two principal mechanism of shear stress-dependent endothelial autocoid release, Am. J. Physiol. 265 (1993) H828–H833.
[9] R.A. Cohen, P.M. Vanhoutte, Endothelium-dependent hyperpolarization, Circulation 92 (1995) 3337–3349.
[10] O.P. Hamill, D.W. Mcbride, The pharmacology of mechanogated membrane ion channels, Pharmacol. Rev. 48 (1996) 231–252.
[11] M. Sansom, The biophysics of peptide models of ion channel, Prog. Biophys. Mol. Biol. 55 (1991) 139–235.
[12] L.R. Opsahl, W.W. Webb, Transduction of membrane tension by the ion channel alamethicin, Biophys. J. 66 (1994) 71–74.
[13] E. Bedard, C.E. Morris, Channel activated by stretch in neurons of helix snail, Can. J. Physiol. Pharmacol. 70 (1992) 207–213.
[14] X. Yao, H.Y. Kwan, F.L. Chan, N.W.K. Chan, Y. Huang, A protein kinase G-sensitive channel mediates flow-induced Ca^{2+} entry in vascular endothelial cells, FASEB J. 14 (2000) 932–938.
[15] J.D. Pearson, J.S. Carleton, A. Hunchings, J.L. Gordon, Uptake and metabolism of adenosine by pig aortic endothelial and smooth-muscle cells in culture, Biochem. J. 170 (1978) 265–271.
[16] O.P. Hamill, A. Marty, B. Sakmann, F.J. Sigworth, Improved patch-clamp techniques for high-resolution current recording from cells and cell-free membrane patches, Pflug. Arch. 391 (1981) 85–100.
[17] S.J. Beebe, J.D. Corbin, Cyclic nucleotide-dependent protein kinases, in: P.D. Boyer, E.G. Krebs (Eds.), The Enzymes, vol. 17, Academic Press, New York, 1986, pp. 43–106.
[18] C.A. Lewis, Ion-concentration dependence of the reversal potential and the single channel conductance of ion channels at the frog neuromuscular junction, J. Physiol. 286 (1979) 417–445.
[19] Y. Yamamoto, G. Chen, K. Miwa, H. Suzuki, Permeability and Mg^{2+} blockade of histamine-operated cation channel in endothelial cells of rat intrapulmonary artery, J. Physiol. 450 (1992) 395–408.
[20] T.M. Griffith, Endothelium-derived relaxing factor and the control of flow in conduit and resistance arteries, in: J.A. Bevan, G. Kaley, G.M. Rubanyi (Eds.), Flow-dependent Regulation of Vascular Function, Oxford University Press, Oxford, 1995, pp. 178–213.
[21] J.F. Falcone, L. Kuo, G.A. Meininger, Endothelial call calcium increases during flow-induced dilation in isolated arterioles, Am. J. Physiol. 264 (1993) H653–H659.
[22] G. Helmlinger, B.C. Berk, R.M. Nerem, Pulsatile and steady flow-induced calcium oscillations in single cultured endothelial cells, J. Vasc. Res. 33 (1996) 360–369.
[23] G. Schwarz, G. Callewaert, G. Droogmans, B. Nilius, Shear stress-induced calcium transients in endothelial cells from human umbilical cord veins, J. Physiol. 458 (1992) 527–538.
[24] O.P. Hamill, D.W. McBride, Rapid adaptation of a single mechanosensitive channels in *Xenopus* oocytes, Proc. Natl. Acad. Sci. USA 89 (1992) 7462–7466.
[25] C.E. Morris, R. Horn, Failure to elicit neuronal macroscopic mechanosensitive currents anticipated by single-channel studies, Science 251 (1991) 1246–1249.
[26] I.V. Tabarean, P. Juranka, C.E. Morris, Membrane stretch affects gating modes of a skeletal muscle sodium channel, Biophys. J. 77 (1999) 758–774.
[27] F. Sachs, Mechanical transduction in biological systems, Crit. Rev. Biomed. Eng. 16 (1988) 141–169.
[28] J.L. Balligand, P.J. Cannon, Nitric oxide synthases and cardiac muscle. Autocrine and paracrine influences, Arterioscler. Thromb. Vasc. Biol. 17 (1997) 1846–1858.
[29] M.P. Murphy, Nitric oxide and cell death, Biochim. Biophys. Acta 1411 (1999) 401–414.
[30] X.D. Wan, P. Juranka, C.E. Morris, Activation of mechanosensitive currents in traumatized membrane, Am. J. Physiol. 276 (1999) C318–C327.